Evidence for growing structural correlation length in colloidal supercooled liquids

Jiankai Hu,[1,2] Luhui Ning,[1,2] Rui Liu,[1] Mingcheng Yang,[1,2,3] and Ke Chen[1,2,3,*]

[1]*Beijing National Laboratory for Condensed Matter Physics and Key Laboratory of Soft Matter Physics, Institute of Physics, Chinese Academy of Sciences, Beijing 100190, China*

[2]*University of Chinese Academy of Sciences, Beijing 100049, China*

[3]*Songshan Lake Materials Laboratory, Dongguan, Guangdong 523808, China*

(Received 21 April 2022; accepted 3 October 2022; published 4 November 2022)

Using video microscopy, we measure the long-time diffusion coefficients of colloidal particles at different concentrations. The measured diffusion coefficients start to deviate from theoretical predictions based on random collision models upon entering the supercooled regime. The theoretical diffusion relation is recovered by assigning an effective mass proportional to the size of structurally correlated clusters to the diffusing particles, providing an indirect method to probe the growth of static correlation length scales approaching the glass transition. This method is tested and validated in the crystallization of mono-disperse colloids in quasi-two-dimensional experiments. The correlation length obtained for a binary colloidal liquid increases by a power law toward a critical packing fraction of ∼0.79. The system relaxation time exhibits a power-law dependence on the correlation length in agreement with dynamical facilitation theories.

DOI: 10.1103/PhysRevE.106.054601

Glass transition is one of the most intriguing problems in physics. A longstanding question about glass transition is, "what is the structural origin for the drastic slowdown of the dynamics near the glass transition?" The Adam-Gibbs theory suggests that the relaxation process in supercooled liquids is determined by the activation energy of the cooperative regions [1]. As the temperature is lowered, the activation barrier increases with the size of the cooperative region. Along this line, motivated by mean-field theories of structural glass transition [2–7], random first-order transition theories (RFOT) associate the slowing down of the dynamics to the emergence and growth of a static structural length scale [8–13], which is the characteristic size of low-entropy droplets.

Many theoretical efforts have been made to detect the growth of the structurally correlated clusters in liquids and glasses. Tanaka *et al.* find that the characteristic length scale of the medium-range crystalline order (MRCO) follows an Ising-like power-law divergence towards the glass transition in polydisperse supercooled liquids [14]. Under the condition of the isoconfigurational average, Tong *et al.* show that the length scale of sterically favored structures grows coherently with the dynamical length scales in liquids [15]. Karmakar *et al.* perform finite size scaling analyses for the Kob-Anderson Lennard-Jones model to extract a temperature-dependent static length scale $\xi_s(T)$ for the structural entropy, which determines the structural relaxation time in glasses [16]. Structural correlation length can also be estimated by examining elastic vibration modes of systems of different sizes at low temperatures, which is found to be proportional to $\xi_s(T)$ [17]. Point-to-set (PTS) theory provides a quantitative method to probe the static correlation length scale by examining the effect of a field of pinned particles on the dynamics of neighboring particles [18]. The dynamics of an unpinned particle becomes arrested when it is within the range of the static length scale to a pinned field. Using the PTS approach, recent simulations observe the growth of static correlation length scales in supercooled liquids under different pinning patterns [19–22], with the α-relaxation time increasing exponentially with the static correlation length.

Generally, the measurements of static structural correlation length in liquids or glasses require either specific knowledge of the order probed, which is far from obvious for amorphous systems, or stringent conditions that are difficult to fully realize in experiments, such as selectively pinning particles in a thermal environment. As a result, there are relatively few reports of experimental measurements of the structural correlations in glassy systems. Recent experiments of colloidal particles confined in spherical cavities show a divergent static length scale near a critical packing fraction [23]. Using optical tweezers, experiments in a 2D colloidal system observe a slow increase of the PTS static length scale near a wall of pinned particles [24].

In this paper, we propose an alternative method to indirectly detect the growth of correlated structures in supercooled liquids without the need for pinning particles in experiments. This method is based on the hypothesis that a diffusing colloidal particle in a structurally correlated cluster acquires an effective mass proportional to the size of the cluster. After this effective mass has been properly accounted for, the long-time diffusion coefficient D of the particles can then be described by the universal diffusion relation based on random collision models [25,26],

$$D = \frac{k_B T}{A\xi_B(1 - S_2) + \xi_s}. \tag{1}$$

Here, $k_B T$ is the thermal energy, ξ_B is the binary collision friction in the Enskog gas theory, S_2 is the two-body excess

*kechen@iphy.ac.cn

entropy, ξ_s is the solvent friction, and A is a fitting parameter independent of the system packing fractions. An averaged static length scale can be extracted from the effective mass of structurally correlated clusters.

Using this method, we measure the long-time diffusion coefficients of colloidal particles in normal and supercooled liquids in quasi-two-dimensional (quasi-2D) configurations. The measured diffusion coefficients begin to deviate from Eq. (1) as the system enters the supercooled stage, signaling the emergence of correlated structures. The extracted structural correlation length grows with the packing fraction by a power-law function with respect to a critical packing fraction of ∼0.79. And the α-relaxation time of the system increases with this correlation length by a power law, which implies weaker-than-expected structural correlations before the glass transition. We test and validate our method by measuring the structural correlation length during the crystallization of colloids at 2D before the hexatic phase transition, where the growth of the structurally correlated clusters and diffusion coefficients can be independently measured. The correlation length extracted from the diffusion coefficient during crystallization increases linearly with the size of crystallites as well as the spatial correlation length of bond orientational orders. The static correlation length increases exponentially with the packing fraction as predicted by the KTHNY theory [27–31].

The samples consist of a binary mixture of poly-N-isopropylacrylamide (PNIPAM) particles confined between two coverslips, forming a monolayer. The particle diameters are 1.2 μm for large particles and 0.9 μm for small particles, respectively, measured by dynamical light scattering (DLS) at 24 °C. The number ratio between the two species is tuned to be ∼1.3 to frustrate crystallization at 2D. The packing fraction is adjusted by changing the number density of the samples while keeping the temperature constant at 24 °C. Each sample is equilibrated on the microscope stage for at least one hour before being continuously imaged using standard bright field microscopy at 60 fps. Depending on the sample packing fraction, videos from 3 to 17 minutes are acquired so that the long-time diffusion coefficients of the particles can be properly determined. The trajectories of all particles are extracted using particle tracking software [32]. Diffusion coefficients are determined by linearly fitting the long-time mean square displacements (MSDs) of the particles using $MSD = 4Dt$. For comparison, similar measurements are performed for monodispersed samples before the hexatic stage of crystallization at 2D.

As the packing fraction increases, the system becomes supercooled, characterized by the intermediate scattering function (ISF) with $ISF = \frac{1}{N}\langle\sum_i e^{i\frac{2\pi}{a}(\mathbf{r}_i(t)-\mathbf{r}_i(0))}\rangle$ [33,34]. Here, a is the first peak's position of the radial distribution function $g(r)$, $\mathbf{r}_i(t)$ is the position of particle i at time t, N is the number of particles, and $\langle\cdots\rangle$ represents time average. The ISFs are obtained after the Mermin-Wagner fluctuations are removed using cage-relative displacements corrections [35–37]. Figure 1(a) plots the measured intermediate scattering function of the samples at different packing fractions. The α-relaxation time τ_α is determined as the time interval at which ISF drops to $1/e$. Figure 1(b) plots the τ_α as a function of the packing fraction. At low packing fractions, τ_α can be well fitted to the Arrhenius function. For packing fractions higher than 0.55, τ_α starts to deviate from the Arrhenius function and increases dramatically, a signature of supercooled liquids [38,39].

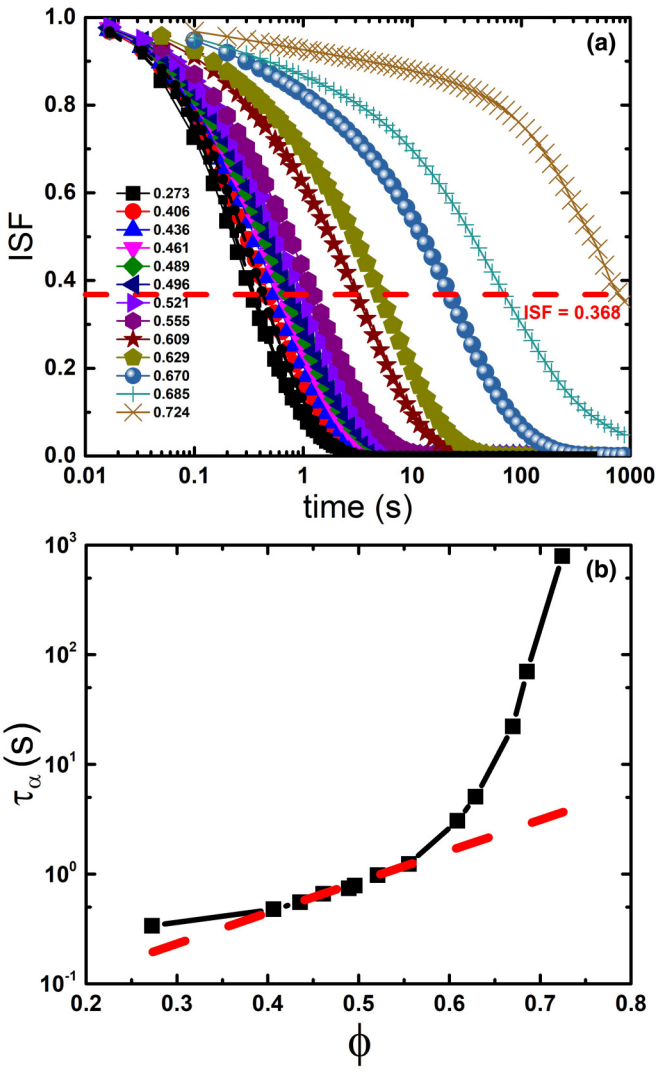

FIG. 1. (a) Intermediate scattering functions (ISFs) at packing fractions ranging from 0.273 to 0.724. The red dashed line is $ISF = 1/e$. (b) The alpha-relaxation time τ_α acquired from (a). The red dashed line is an Arrhenius fitting. τ_α starts to deviate the Arrhenius function and increases dramatically for packing fractions higher than 0.55, indicating that the system becomes supercooled.

Figure 2(a) plots the measured diffusion coefficients D for both large and small particles at different packing fractions. At low packing fractions, D can be well fitted by Eq. (1), which suggests that the diffusion process can be described by random collision models, with no significant spatial or temporal correlations. The measured diffusion coefficients become considerably lower than theoretical predictions at the packing fraction of the onset of the supercooled regime determined by τ_α. Similar breakdowns of theoretical models for diffusion coefficients have been reported in ellipsoidal and spherical colloidal experiments by Li *et al* [40].

The slowing down of the diffusing dynamics can be attributed to the emergence of correlated structures in the

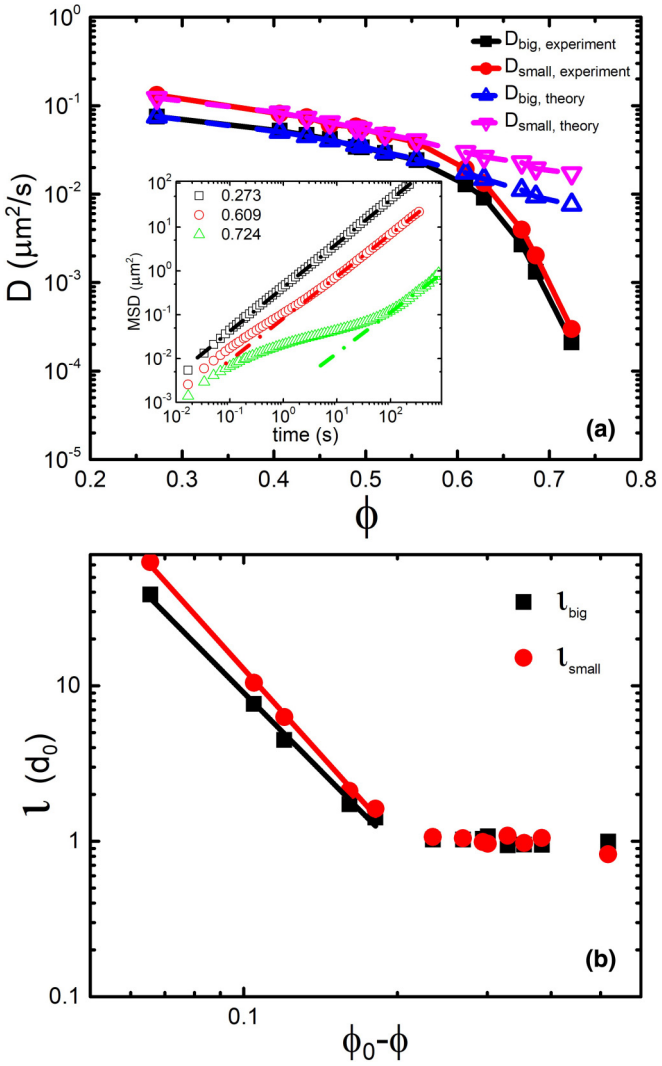

FIG. 2. (a) Measured (solid symbols) and theoretical (empty symbols) diffusion coefficients for both large and small particles as a function of packing fraction. The experimental measurements deviate from theoretical predictions for packing fractions higher than 0.55 at the onset of the supercooled regime. Inset: Representative mean square displacement curves at different packing fractions with linear fitting for the long time MSDs (dashed lines). (b) Static correlation length l for both the large and small particles as a function of packing fraction. Solid lines are fit to a power law function($l \propto (\phi_0 - \phi)^{-\gamma}$) for the experimental data with $\phi > 0.55$, with $\gamma_{\text{big}} = 3.3 \pm 0.83$, $\phi_{0,\text{big}} = 0.79 \pm 0.03$, and $\gamma_{\text{small}} = 3.74 \pm 0.59$, $\phi_{0,\text{small}} = 0.79 \pm 0.02$.

supercooled liquid. As the particles in a statically correlated structure must move in unison before the structure relaxes, a correlated cluster can be considered as a diffusing rigid body, with no significant correlations to other clusters. Thus the random collision condition is restored. The long time diffusion behavior of the particles in the system can again be described by Eq. (1). Accordingly, the mass of the diffusing particle m_0 need to be replaced by the mass of the diffusing cluster m_{eff}, which is the total mass of the particles in the cluster, while keeping A constant before and after entering the supercooled regime ($A_{\text{big}} = 1770$ and $A_{\text{small}} = 2146$). The introduction of the effective mass affects the the binary collision friction term $\xi_B = \rho\sigma g(\sigma)\sqrt{2\pi k_B T m_0}$ in Eq. (1). By replacing m_0 with m_{eff}, one obtains $\xi'_B = \rho\sigma g(\sigma)\sqrt{2\pi k_B T m_{\text{eff}}}$ and

$$D_{\text{exp}} = \frac{k_B T}{A\xi'_B(1 - S_2) + \xi_s}. \tag{2}$$

By fitting the experimental data to Eq. (2), the number of particles in a correlated structure can then be estimated as $N = m_{\text{eff}}/m_0$, and a static correlation length $l = \sqrt{N}$ or $l = \xi'_B/\xi_{B,0}$, in the unit of particle diameters d_0, where $\xi_{B,0}$ is the theoretical friction from binary collision of uncorrelated particles. This estimation of the correlation length l is based on the assumption that the shapes of the correlated clusters are compact at 2D, while studies have shown that such clusters may be of fractal dimensions [24,41,42]. Thus our current estimation represents the lower bound of the static length scales, and it properly characterizes the monotonic increase of the size of the correlated clusters, as the system progresses towards colloidal glass transition.

Figure 2(b) plots the measured correlation lengths l as a function of the packing fraction for both large and small particles. At low packing fractions, l is close to unity, indicating no correlated structures in normal liquids. l starts to increase after the system becomes supercooled, and the growth can be fitted to a power-law function with the packing fraction ϕ, namely $l \propto (\phi_0 - \phi)^{-\gamma}$. Within the fitting errors, the fitting parameters are the same for large and small particles, and suggest that the correlation length diverges at a critical packing fraction near $\phi = 0.79$.

To test our hypothesis that the correlation lengths obtained by fitting the diffusion coefficient D to Eq. (2) indeed reflect the size of the structurally correlated clusters, we measure the diffusion coefficients during the crystallization of colloids at 2D, where the size of the ordered structures can be independently quantified. We employ temperature-sensitive PNIPAM particles to tune the packing fraction of the sample from normal liquid to complete crystallization. The analyses are focused on the early stage of the crystallization process before the transition between normal liquid and the hexatic phase at 2D [27–31], when the long-time diffusion coefficients can be obtained experimentally in reasonable time windows. It is also in this stage when orientationally ordered clusters start to emerge from an isotropically disordered liquid.

Similar to the disordered binary samples, the measured diffusion coefficients deviate from theoretical predictions at high packing fractions during crystallization, as plotted in Fig. 3(a). The local crystalline order is characterized by the bond orientational order parameter $\psi_{6,i} = \frac{1}{N}\sum_j e^{i6\theta_{ij}}$, where N is the number of the nearest neighbors to particle i, and θ_{ij} is the bond angle between particle i and its neighbor particle j with respect to a fixed direction (x-axis in the current paper). $\psi_{6,i} = 1$ corresponds to perfect hexagonal local order. We extract the length scale of crystalline clusters l_6 from the spatial correlation function of ψ_6, defined as $g_6(r = |\mathbf{r}_i - \mathbf{r}_j|) = \langle\psi^*_{6,i}(\mathbf{r}_i)\psi_{6,j}(\mathbf{r}_j)\rangle$, which decays exponentially with particle separations by $g_6 \propto e^{-r/l_6}$ before the hexatic phase [25]. We also directly measure the average number of particles N in domains formed by ordered particles. A particle is considered ordered if three or more of its neighbors satisfy the criterion

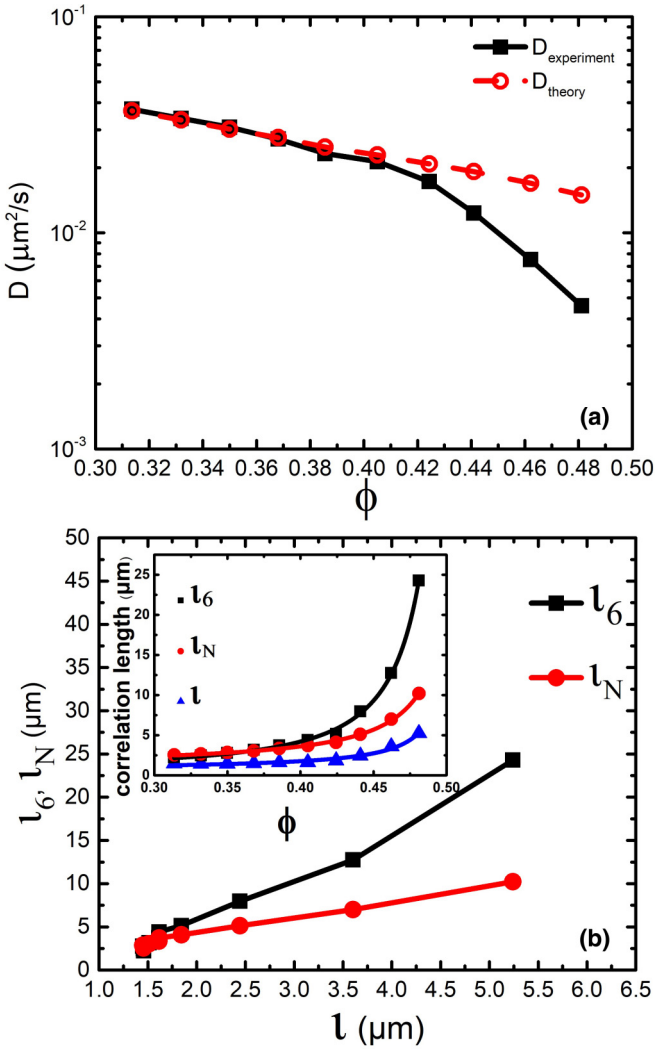

FIG. 3. Measured and theoretical diffusion coefficients for the mono-disperse samples at different packing fractions. The measured diffusion coefficients deviate from theoretical predictions for packing fractions higher than 0.368. (b) Comparison between different length scales, including l_6 extracted from the spatial correlation function g_6 and the size of ordered domains l_N, as a function of l. Inset: the length scales as a function of packing fractions in mono-disperse system before the hexatic transition. The solid lines are fits to the KTHNY prediction $l, l_6, l_N \propto e^{-b/\sqrt{\rho_i-\rho}}$ with $\rho_i = 0.53$.

$|\psi^*_{6,i}\psi_{6,j}| \geqslant 0.65$ [43]. A static correlation length scale is obtained as $l_N = \sqrt{N}$, in the unit of particle diameters. Figure 3(b) plots the static length scales extracted from the spatial correlation functions and direct measurement of the size of ordered domains, as a function of l determined from diffusion coefficients. Both l_6 and l_N increase linearly with l, confirming that l indeed reflects the growth of structurally correlated clusters from isotropic liquids. All three correlation lengths, l, l_6, and l_N increase with the packing fraction by $e^{-b/\sqrt{\rho_i-\rho}}$ as predicted by the KTHNY theory [inset of Fig. 3(b)] [27–31].

We note that the correlation length l is less than both l_6 and l_N in the crystallization experiments. This is because the particles in smaller crystallites have faster dynamics than those in larger ones and contribute more to the measured

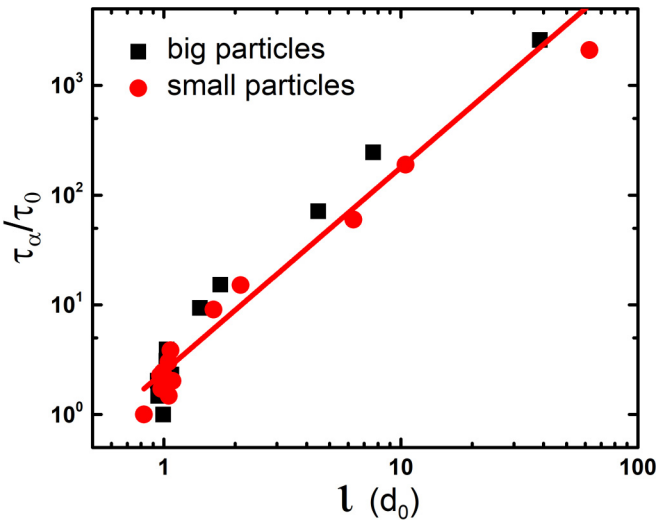

FIG. 4. System relaxation time as a function of structural correlation length l in bi-disperse system (log-log plot). Solid lines represent power law fits ($\tau_\alpha/\tau_0 \propto l^\theta$) to the experimental data for $l > 1$, $\theta = 1.86 \pm 0.08$.

diffusion coefficient. Thus, the diffusion coefficient reflects an average domain size smaller than the mean size of all the crystalline clusters in the system, an effect that also impacts the correlation lengths obtained in binary fluids. Nevertheless, the proportionality between the three correlation lengths suggests that l indeed measures the growth of structural orders in liquids.

In the crystallization experiments, the observation range is limited by the size of the field of view and the dynamics in the system. As the packing fraction continues to increase, the crystalline domains soon percolate the field of view and the dynamic slows down considerably, preventing proper measurements of structural correlation lengths or the long-time diffusion coefficients.

For the binary fluids, the system relaxation time increases with the growth of the correlation length. Figure 4 plots the system relaxation time τ_α/τ_0 as a function of the correlation lengths for a binary system, where τ_0 is the α-relaxation time at the lowest packing fraction. The relaxation times for both the large and small particles follow a power law function after the onset of the supercooled regime when $l > 1$. The power index is 1.86 ± 0.08 for both species. The observed powerlaw increase of the relaxation time with the structural correlation length is not in agreement with the activated dynamics of RFOT models that predict an exponential increase of τ_α. The observations in experiments imply that the ordered structures formed in the supercooled liquids have weaker static correlations than that expected by RFOT, and the relaxation barrier does not increase proportionally with the cluster size.

The power law relation between τ_α and l can be understood by dynamical facilitation models. As the packing fractions in our experiments are limited by the need to measure the long time diffusion coefficient, when the MSD reaches the linear regime, most of our samples are below a crossover packing fraction determined by mode coupling theories where the

dynamics are dominated by dynamical facilitation [24,44]. The crossover packing fraction $\phi_{\mathrm{MCT}} = 0.70$, obtained by fitting the τ_α to the packing fraction by $\tau_\alpha \propto (1/\phi - 1/\phi_{\mathrm{MCT}})^{\gamma_{\mathrm{MCT}}}$, is close to the highest packing fraction of 0.724 in our experiments. Kinetically constrained theories [45–48] predict a power law increase of τ_α with the characteristic separations between defect (mobile) particles. Even though the kinetically constrained models do not explicitly require the nucleation of droplets as in the RFOT, the defect particles can be viewed as separated by correlated domains.

In conclusion, we recover the universal diffusion relation based on random collision models by associating the size of structurally correlated domains to the effective mass of diffusing particles in supercooled liquids, providing an indirect way to probe the growth of static structural correlation length scales in supercooled liquids or glasses without the need for selectively pinning particles. The correlation lengths thus obtained agrees qualitatively with theoretical models, and the method is independently validated in the crystallization of colloids at 2D. More information regarding the development of dynamical heterogeneity in supercooled liquids may be revealed if the distributions of the cluster sizes and the corresponding relaxation times can be included in a refined model.

We acknowledges support from National Natural Science Foundation of China (Grants No. 12174434 and No. 11874395). This work was also supported by the Strategic Priority Research Program of Chinese Academy of Sciences (Grant No. XDB33000000).

[1] G. Adam and J. H. Gibbs, J. Chem. Phys. **43**, 139 (1965).
[2] Y. Singh, J. P. Stoessel, and P. G. Wolynes, Phys. Rev. Lett. **54**, 1059 (1985).
[3] T. R. Kirkpatrick and P. G. Wolynes, Phys. Rev. A **35**, 3072 (1987).
[4] T. Kirkpatrick and D. Thirumalai, J. Phys. A: Math. Gen. **22**, L149 (1989).
[5] T. R. Kirkpatrick and P. G. Wolynes, Phys. Rev. B **36**, 8552 (1987).
[6] T. R. Kirkpatrick and D. Thirumalai, Phys. Rev. B **37**, 5342 (1988).
[7] T. R. Kirkpatrick and D. Thirumalai, Phys. Rev. Lett. **58**, 2091 (1987).
[8] T. R. Kirkpatrick, D. Thirumalai, and P. G. Wolynes, Phys. Rev. A **40**, 1045 (1989).
[9] L. Berthier and G. Biroli, Rev. Mod. Phys. **83**, 587 (2011).
[10] V. Lubchenko and P. G. Wolynes, Annu. Rev. Phys. Chem. **58**, 235 (2007).
[11] P. G. Wolynes, J. Res. Natl. Inst. Stand. Technol. **102**, 187 (1997).
[12] X. Xia and P. G. Wolynes, Phys. Rev. Lett. **86**, 5526 (2001).
[13] V. Lubchenko and P. G. Wolynes, J. Chem. Phys. **119**, 9088 (2003).
[14] H. Tanaka, T. Kawasaki, H. Shintani, and K. Watanabe, Nat. Mater. **9**, 324 (2010).
[15] H. Tong and H. Tanaka, Phys. Rev. X **8**, 011041 (2018).
[16] S. Karmakar, C. Dasgupta, and S. Sastry, Proc. Natl. Acad. Sci. **106**, 3675 (2009).
[17] S. Karmakar, E. Lerner, and I. Procaccia, Physica A **391**, 1001 (2012).
[18] J.-P. Bouchaud and G. Biroli, J. Chem. Phys. **121**, 7347 (2004).
[19] G. Biroli, J.-P. Bouchaud, A. Cavagna, T. S. Grigera, and P. Verrocchio, Nat. Phys. **4**, 771 (2008).
[20] G. M. Hocky, T. E. Markland, and D. R. Reichman, Phys. Rev. Lett. **108**, 225506 (2012).
[21] L. Berthier and W. Kob, Phys. Rev. E **85**, 011102 (2012).
[22] W. Kob and L. Berthier, Phys. Rev. Lett. **110**, 245702 (2013).
[23] B. Zhang and X. Cheng, Phys. Rev. Lett. **116**, 098302 (2016).
[24] K. H. Nagamanasa, S. Gokhale, A. Sood, and R. Ganapathy, Nat. Phys. **11**, 403 (2015).
[25] A. Samanta, Sk. Musharaf Ali, and S. K. Ghosh, Phys. Rev. Lett. **92**, 145901 (2004).
[26] L. Ning, P. Liu, Y. Zong, R. Liu, M. Yang, and K. Chen, Phys. Rev. Lett. **122**, 178002 (2019).
[27] J. M. Kosterlitz and D. J. Thouless, J. Phys. C: Solid State Phys. **6**, 1181 (1973).
[28] D. R. Nelson and B. I. Halperin, Phys. Rev. B **19**, 2457 (1979).
[29] A. Young, Phys. Rev. B **19**, 1855 (1979).
[30] Y. Han, N. Y. Ha, A. M. Alsayed, and A. G. Yodh, Phys. Rev. E **77**, 041406 (2008).
[31] D. R. Nelson, *Defects and Geometry in Condensed Matter Physics* (Cambridge University Press, Cambridge, 2002).
[32] J. C. Crocker and D. G. Grier, J. Colloid Interface Sci. **179**, 298 (1996).
[33] J. Horbach and W. Kob, Phys. Rev. E **64**, 041503 (2001).
[34] T. Kawasaki and H. Tanaka, Phys. Rev. E **89**, 062315 (2014).
[35] H. Shiba, Y. Yamada, T. Kawasaki, and K. Kim, Phys. Rev. Lett. **117**, 245701 (2016).
[36] B. Illing, S. Fritschi, H. Kaiser, C. L. Klix, G. Maret, and P. Keim, Proc. Natl. Acad. Sci. **114**, 1856 (2017).
[37] S. Vivek, C. P. Kelleher, P. M. Chaikin, and E. R. Weeks, Proc. Natl. Acad. Sci. **114**, 1850 (2017).
[38] P. G. Debenedetti and F. H. Stillinger, Nature (London) **410**, 259 (2001).
[39] G. Brambilla, D. El Masri, M. Pierno, L. Berthier, L. Cipelletti, G. Petekidis, and A. B. Schofield, Phys. Rev. Lett. **102**, 085703 (2009).
[40] B. Li, X. Xiao, K. Lou, S. Wang, W. Wen, and Z. Wang, Commun. Phys. **1**, 79 (2018).
[41] J. D. Stevenson, J. Schmalian, and P. G. Wolynes, Nat. Phys. **2**, 268 (2006).
[42] J. D. Stevenson and P. G. Wolynes, Nat. Phys. **6**, 62 (2010).
[43] H. Zhang and Y. Han, Phys. Rev. X **8**, 041023 (2018).
[44] S. M. Bhattacharyya, B. Bagchi, and P. G. Wolynes, Proc. Natl. Acad. Sci. **105**, 16077 (2008).
[45] J. P. Garrahan and D. Chandler, Phys. Rev. Lett. **89**, 035704 (2002).
[46] C. Toninelli, G. Biroli, and D. S. Fisher, Phys. Rev. Lett. **92**, 185504 (2004).
[47] S. Whitelam, L. Berthier, and J. P. Garrahan, Phys. Rev. Lett. **92**, 185705 (2004).
[48] F. Ritort and P. Sollich, Adv. Phys. **52**, 219 (2003).